Reliability Engineering and System Safety 253 (2025) 110524

Contents lists available at ScienceDirect

Reliability Engineering and System Safety

journal homepage: www.elsevier.com/locate/ress

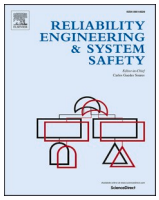

Reliability modeling of multi-state phased mission systems with random phase durations and dynamic combined phases

Xiang-Yu Li [a], He Li [b,*], Xiaoyan Xiong [a], Mingwei Li [c], Mohammad Yazdi [d], Esmaeil Zarei [e]

[a] Key Laboratory of Advanced Transducers and Intelligent Control System, Ministry of Education, Taiyuan University of Technology, 030024, Taiyuan, China
[b] Centre for Marine Technology and Ocean Engineering (CENTEC), Instituto Superior Técnico, Universidade de Lisboa, Lisbon, Portugal
[c] College of Shipbuilding Engineering, Harbin Engineering University, Harbin, China
[d] School of Engineering, Macquarie University, Sydney, Australia
[e] Department of Safety Science and Robertson Safety Institute (RSI), College of Aviation, Embry-Riddle Aeronautical University, Prescott, AZ 86301, USA

ARTICLE INFO

Keywords:
Reliability Modeling, Multistate Phased Mission System
Dynamic phase combination
Random Phase Durations

ABSTRACT

Random phase durations and dynamic combined phases challenge the application of existing reliability models in the reliability analysis of multistate-phased mission systems (MS-PMSs). To this end, this paper presents a new reliability modeling method for multi-state phased mission systems with random phase durations and dynamic combined phases. Initially, a multi-state multi-valued decision diagram-based (MMDD-based) reliability modeling method is created to efficiently map random phase durations and the dynamic combined phase nature of MS-PMSs into the reliability model. To solve the MMDD-based reliability model, a path probability evaluation method is subsequently constructed with the assistance of the Markov regenerative function. The effectiveness and the superior performance of the proposed MMDD-based reliability model and its solving algorithm are validated by the application to the reliability modeling and analysis of an attitude and orbit control system with multiple modes. Overall, this paper provides the reliability sector with a new reliability model and its solving algorithm to enhance the reliability and safety of multi-state phased mission systems.

1. Introduction

The whole mission of Phased Mission Systems (PMSs), such as manned spaceflight [1], satellite [2], aviation flight [3], as well as nuclear power [4], can be divided into several subtasks, which are completed in a series and continuous time durations, called phases. PMSs accomplishes a series of missions in their whole lifelong with diverse failure criteria and working environment [2]. For instance, the full mission of a flight includes taxi and take-off, cruise, and landing. Each phase requires specific power and experiences unique working conditions. The dynamic behaviors raise difficulties in PMSs reliability modeling, that is to assesss the reliability and safety of whole PMSs, which, however, is challenging with the consideration of phase dependencies [5].

Most methods for PMSs reliability modeling are developed based on ordinary modeling concepts. These methods include: (i) The combinatorial methods based on static models, for instance, fault tree [6] and decision diagram-based methods [7], deal with reliability modeling of large-scale PMSs with improved modeling efficiency; (ii) The state space-based models, like the Markov process [8], are able to map dynamic characters of elements within phases such as cold spare components [9], dependent failure [10], etc.; (iii) The modular methods or the hierarchical models combine the two concepts already mentioned and take all their advantages [11]. Furthermore, the classification of PMSs into distinct groups is informed by their system characteristics, encompassing aspects such as phase AND/OR/Dynamic, the utilization of static methods versus state space models, binary versus multistate systems, the nature of phase durations (fixed or random), and the underlying statistical distributions (exponential or random), see Table 1. The contributions of methods are categorized into: complexity, efficiency, and a combination of both, offering a structured overview of the previous models.

Table 1 reveals that a majority of the existing methodologies operate under two assumptions:

(i) Static phases, implying that the sequence in phases is executed remains unchanged. Static phases do not align with the reality of certain PMSs, where the operational procedures are inherently dynamic. A prime example of this dynamism is observed in the attitude

* Corresponding author.
E-mail address: he.li@centec.tecnico.ulisboa.pt (H. Li).

https://doi.org/10.1016/j.ress.2024.110524
Received 5 April 2024; Received in revised form 25 August 2024; Accepted 30 September 2024
Available online 15 October 2024

Notations

A_i	Component A in phase i.
$A_{i,j}$	Component A is in state j in phase i.
$index(A_i)$	The order of variable A_i.
T_i	The phase duration of phase i
Pi_j	The end state of phase i is j.
η_i^M	The ith mission path.
η_i^C	The ith component path.
$F_{i,j}(t)$	The distribution of component state transition time from state i to state j.
$\boldsymbol{Q}(t)$	The kernel matrix
$\boldsymbol{\theta}(t)$	The state transition probability matrix
$f_{T_i}(t)$	The probability density function of phase duration T_i
s_i	The component state at the end of phase i
α, β	The shape parameter and scale parameter for the Weibull distribution

Acronym

BDD	Binary decision diagram
FT	Fault tree
MMDD	Multi-state multivalued decision diagram
PDO	Phase dependent operation
PMS	Phased mission system
PMS-BDD	BDD model for phased mission system
PMS-MMDD	MMDD model for phased mission system

control systems of satellites, as illustrated in Fig. 1. In Fig. 1, the numbers 2, 1 and 0 represent three states for the missions (success, degrade and failure). As we can see from Fig. 1, the failure of one mission may not lead to direct failure of the whole mission. The dynamic characteristics are shown in two aspects: (1) The phases executed are decided by the result of former phases; (2) Some missions could be re-executed. For example, if the 'Firing and adjusting' mission fails, the whole mission will be re-executed if there are enough redundant working components and fuel. These systems must adapt their operational strategy in a real-time mode based on external conditions and mission requirements, showcasing a level of flexibility and responsiveness that static phase assumptions fail to capture.

Dynamic phase combinations, if some missions fail or are not ideal, the phases executed are different, see Fig. 1. The backup mission mechanism has been considered. For instance, Yu et al. [21] proposed a Binary decision diagram (BDD)-based method to model the PMS with backup missions, in which the system could re-execute missions to improve system reliability. Li et al. [25] introduced a multistate multi-valued decision diagram (MMDD)-based method to model PMSs with backup missions, which can efficiently model PMSs with multistate components. Wang et al. [30] considered the PMS with backup missions and system risks simultaneously and the mission success probabilities are used as an objective to optimize the system reliability. Li et al. [31] considered the backup mission mechanisms in MS-PMSs and proposed a mixed redundancy strategy for system optimization. Wu et al. [32,33] studied the PMS with backup missions, and an improved BDD model is also proposed for system reliability evaluation. All research above considered the backup mission only triggered after failed normal missions. In the present research, however, a more general mechanism is considered when the mission result is not ideal (not failed), extra missions will be executed for a higher precision. And mission failure is another special case in this model. And an improved PMS-MMDD model is proposed for reliability modeling.

(ii) The fixed phase duration. Most existing methods assume that the phase durations are fixed, which is against the practice. The phase durations are affected by many factors, such as external environment, personnel operation level, etc. Only a few studies considered the mentioned scenarios. To be specific, Jia et al. [20] proposed a simulation-based PMS reliability modeling concept with the consideration of common cause failures and random phase durations The method can improve the accuracy of the result by a more close-to-practice modeling technique. Mo et al. [34] proposed a Markov regenerative process-based method to model fault-tolerant PMSs with random phase durations, which can better map the uncertain nature of phases. The simulation-based methods are time-consuming. To this end, new ideas to evaluate the system reliability, incorporating the Markov renewal theory are necessary by the sector.

To deal with the problems mentioned above, a reliability modeling

Table 1
Reliability modeling methods of phased mission systems.

	Phase Combination			Modeling Methods		Binary/ Multistate PMS		Phase Duration		Component Failure Distribution		*Article Contributions*		
	AND	*OR*	*Dynamic*	*Static*	*State space*	*Binary*	*MS*	*Fixed*	*Random*	*Exp*	*Random*	*Complexity*	*Efficiency*	*Both*
[8] Kim, 1994	√				√	√		√		√		■		
[13] Tang, 2006	√			√		√		√		√		■		
[14] Xing, 2007	√			√		√		√		√		■		
[18] Wu, 2018	√			√		√		√		√		■		
[19] Li, 2018	√			√	√	√		√			√	■		
[20] Jia, 2019	√				√	√			√	√		■		
[21] Levitin, 2020	√				√	√		√		√		■		
[23] Cheng, 2021	√				√		√	√		√		■		
[24] Mura, 2021	√				√	√		√		√		■		
[25] Li, 2022			√	√	√		√	√			√	■		
[27] Coolen, 2020	√				√	√		√			√	■		
[28] Tang, 2023			√	√		√		√			√	■		
[29] Levitin, 2015	√			√		√			√		√	■		
[7] Zang, 1999	√			√		√		√		√			■	
[15] Amri, 2018	√			√		√		√			√		■	
[16] Peng, 2014	√			√		√		√		√			■	
[17] Lu, 2018	√			√		√		√		√			■	
[22] Wang, 2020	√			√		√		√		√			■	
[26] Wang, 2023	√			√		√		√		√			■	
[12] Xing, 2002		√		√		√		√		√				■

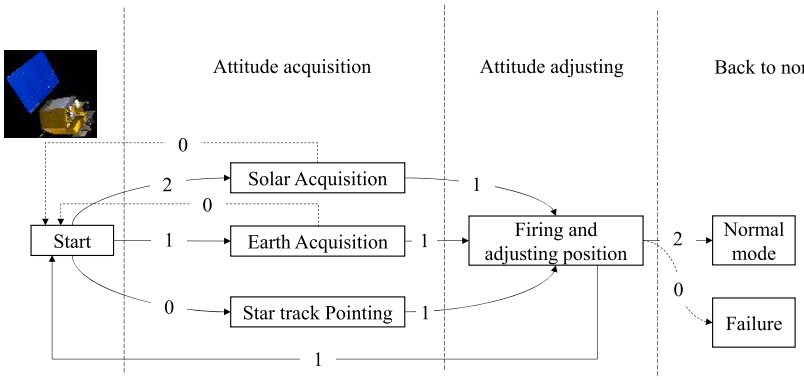

Fig. 1. The mission execution process of one attitude control process of a satellite.

mechanism including multi-state multi-valued decision diagram-based (MMDD-based) reliability modeling and the Markov renewal equation-based model solving method are proposed. The novelties of the paper are as follows:

(i) Construct a reliability modeling method and its corresponding solving algorithm for MS-PMS with random phase durations and dynamic combined phases.
(ii) Extend the MMDD manipulation rule as a basis to model the MS-PMS with dynamic phase combinations.
(iii) Propose a Markov renewal equation-based evaluation method based on the constructed MMDD model to compute the path probability, considering both the non-exponential multistate components and random phase durations.

The rest of the article is organized as follows. Concepts and assumptions are introduced in Section 2. Section 3 presents the method for system MMDD model construction. Section 4 proposes the Markov renewal equation-based path probability evaluation method. The case study is illustrated in Section 5. Section 6 provides conclusions.

2. Concepts and assumptions

Assumptions are presented as follows.

(1) There are n components and each with $m+1$ states.
(2) Components are independent (degrade along with the mission execution) and unrepairable during the missions.
(3) The multiple system states (at the end of phases) are decided by that of components.
(4) Different phases are combined to complete missions that cannot be simply modeled by AND or OR logic.
(5) Some mission durations are uncertain and follow specific distributions, i.e., the normal distribution.

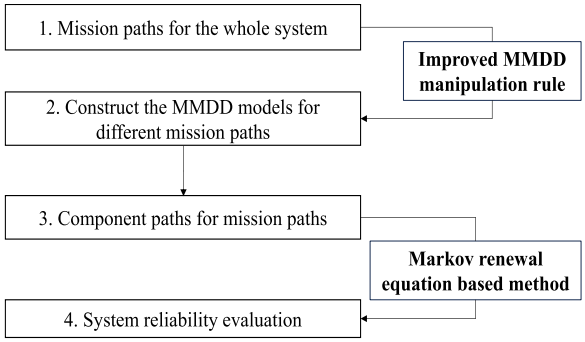

Fig. 2. Mission execution procedure of the example MS-PMS.

The system evaluation mechanism and procedure are shown in Fig. 2.

3. MS-PMS modeling with dynamic phase combinations

3.1. MMDD

The MMDD method is an upgraded version of the BDD. Two output variables (occurrence and nonoccurrence) for each nonterminal node in BDD models but it becomes multiple in MMDD, representing multiple possible results of multistate systems. For example, if component A has m states, $[m, m-1, \cdots, 1]$, and it is in state $j(m>j>1)$ in phase i, its mathematical expression is $A_{i,j} = case(A_i, \underbrace{0, \cdots, 0}_{m-j}, 1, \underbrace{0, \cdots, 0}_{j-1})$. In this *case* expression, A_i represents that component A is in phase i. '1' and '0' represent variable A_i is in and not in this particular state, respectively. The graphic representation is shown in Fig. 3.

In Fig. 3, 'm+1', 'j' and '0' embed in the lines represent the states of variable A_i. '1' and '0' in the circles correspond to the '1' and '0' in the *case* expression, representing variable A_i is in and not in this state. The integration of multiple MMDD models is based on the MMDD manipulation rules, shown as:

$$g \blacklozenge h = case(x, G_1, \cdots, G_m) \blacklozenge case(y, H_1, \cdots, H_m) = \begin{cases} case(x, G_1 \blacklozenge H_1, \cdots, G_m \blacklozenge H_m) & index(x) = index(y) \\ case(x, G_1 \blacklozenge h, \cdots, G_m \blacklozenge h) & index(x) < index(y) \\ case(y, g \blacklozenge H_1, \cdots, g \blacklozenge H_m) & index(x) > index(y) \end{cases} \quad (1)$$

where, $g = case(x, G_1, \cdots, G_m)$ and $h = case(y, H_1, \cdots, H_m)$ represent two variables and $\blacklozenge$ is the logic operation 'AND' or 'OR'. G_i and H_i are variables that represent the variable x and y are in state i ($G_i, H_i = 1$) or not ($G_i, H_i = 0$). *index* represents the variable orders, and it is predefined. In the PMS modeling, many systems could not be repaired due their characteristics, such as the spacecraft. Therefore, to consider the non-repairable characteristics, the general *case* manipulation rule of the PMS-MMDD model is modified as:

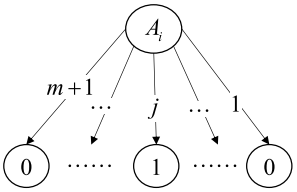

Fig. 3. MMDD model for a multistate component A in any state.

$$G\blacklozenge H = case(A_i, G_m, \cdots, G_1)\blacklozenge case(A_j, H_m, \cdots, H_1)$$
$$= \begin{cases} case(A_i, G_m\blacklozenge E_{j,1}, G_{m-1}\blacklozenge E_{j,2}, \cdots, G_2\blacklozenge E_{j,m-1}, G_1\blacklozenge E_{j,m})\text{Forward } (index(A_i) < index(A_j)) \\ case(A_j, E_{i,m}\blacklozenge H_m, E_{i,m-1}\blacklozenge H_{m-1}, \cdots, E_{i,2}\blacklozenge H_2, E_{i,1}\blacklozenge H_1)\text{Backward}(index(A_j) < index(A_i)) \end{cases} \quad (2)$$
$$E_{i,n} = case\left(A_i, G_m, \cdots, G_n, \underbrace{0, \cdots, 0}_{n-1}\right), E_{j,n} = case\left(A_j, \underbrace{0, \cdots, 0}_{n-1}, H_{m-n+1}, \cdots, H_1\right)$$

In Eq. (2), $G = case(A_i, G_1, \cdots G_m)$ and $H = case(A_j, H_1, \cdots H_m)$ represent the component A in phase i and phase $j(i < j)$. In the forward PDO, the variable ordering is the same as the phase number, $index(A_i) < index(A_j)$, and it is opposite in the backward PDO. In Eq. (2), we can see that all the variables between G_1 and G_{n-1} in $E_{i,n}$ are set to be '0'. The reason is that if variable A_j in state n ($H_n = 1$), which means component A is state n in phase j, component A must be in state n or higher in a former phase i because the component cannot be repaired. Therefore, all the variables between G_1 and G_{n-1} in $E_{i,n}$are set to be '0'. And in $E_{j,n}$ of the forward PDO, the components' state cannot be better in the latter phase. Therefore, all the variables between H_m and H_{m-n} in $E_{j,n}$ are set to be '0'. In this way, the non-repair characteristics is considered in the system modeling, both in backward and forward PDOs. In this way, the non-repair characteristics is considered in the system modeling. It should be noted that, in the PMS-MMDD model, Eq. (1) manipulates the variables representing different components, and Eq. (2) deals with the variables of the same components in different phases.

3.2. MMDD-based PMS modeling with dynamic phase combination

In this section, the MS-PMS with dynamic phase combinations is considered and an MMDD-based method is proposed. A simple PMS example consisting of three missions (M1-M3), six phases (P1-P6), and six components (A-F) is illustrated, and the mission execution procedure is shown in Fig. 4. The solid line and dash lines represent the 'mission success' and 'mission failure', respectively. To be specific, different phases, P2, P3 and P4 will be executed to accomplish mission M2, when the end state of P1 is 2, 1, and 0, respectively. Phase P5 or P6 is selected to accomplish mission M3, according to the mission performance of M2.

For different phases and system states, the working components and system structure functions are also unequal, see Table 2. Components A, C and E with three states (state 2-fully working, state 1-in degradation, and state 0-failure) and others with two (state 1- work and state 0-failure). And the phase durations are T_1, T_2 and T_3, respectively. The structure functions in the 3rd column of Table 2 represent the requirement of the specific phase and states, in which '·' and '+' represent 'AND' and 'OR'. And $A_{i,j}$ represents that component A is in state j in phase i.

The MMDD-based model construction is proposed for the reliability modeling of MS-PMS, as follows:

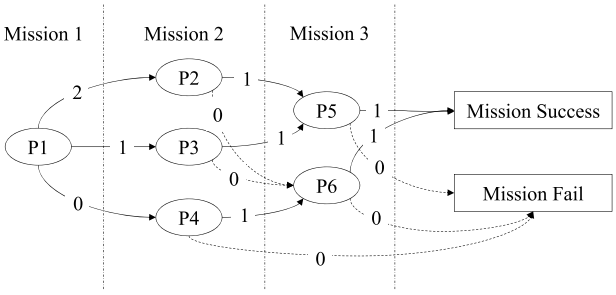

Fig. 4. Mission execution procedure of the MS-PMS.

Step 1. Evaluate the mission paths that lead to mission success, according to the mission execution procedure. For the case shown in Fig. 4, we can see that there are 5 mission paths from phase P1 to mission result 'Mission success', as:

$$\begin{aligned} \eta_1^M &= P1_2P2_1P5_1 \\ \eta_2^M &= P1_2P2_0P6_1 \\ \eta_3^M &= P1_1P3_1P5_1 \\ \eta_4^M &= P1_1P3_0P6_1 \\ \eta_5^M &= P1_0P4_1P6_1 \end{aligned} \quad (3)$$

where, Pi_j represents the system state is in state j at the end of phase i.

Step 2. Construct the MMDD model for different phases and states shown in Table 2. Firstly, the variable order is set to be: $A < B < C < D < E < F$. Then, the MMDD model for different phases and states could be constructed with the general MMDD manipulation rule shown in Eq. (1). Using $P1_2$ as an example, the model construction process is shown in Fig. 5. By this method, the MMDD models for different states of phase P1, $P1_2$, $P1_1$, $P1_0$ are shown in Fig. 6. In the MMDD models, the numbers in the out edges of A_1 represent the state of component A at the end of phase 1. The '1' and '0' in the squares represent whether the system is in this state or not, respectively. The MMDD models for phases and states $P2_1$, $P3_1$ and $P5_1$ are also shown in Fig. 7.

Step 3. Construct the MMDD model for different mission paths. With the mission paths in Eq. (3), the MMDD models for different paths need to be merged into system MMDD model. As some components are used in different phases, and this phase dependency characteristic is dealt with the phase-dependent operation (PDO), both forward and backward. In these two PDO algorithms, the backward PDO is more efficiently, due to its merging features. By the backward PDO, the variables that represent components in different phases could be merged, which could reduce the variable numbers and improve the system modeling efficiency.

Table 2
System structure functions for different phases and system states.

Phases	Missions	States	System structures
P1	1	2	$P1_2 = A_{1,2}\cdot B_{1,1}\cdot C_{1,2}$
		1	$P1_1 = A_{1,2}\cdot B_{1,1}\cdot C_1 + A_{1,1}\cdot B_{1,1}\cdot C_{1,2} + A_{1,1}\cdot B_{1,1}\cdot C_{1,1}$
		0	$P1_0 = A_{1,0} + B_{1,0} + C_{1,0}$
P2	2	1	$P2_1 = A_{2,(2,1)}\cdot D_{2,1}$
		0	$P2_0 = A_{2,0} + D_{2,0}$
P3	2	1	$P3_1 = A_{3,(2,1)}\cdot D_{3,1}\cdot E_{3,(2,1)}$
		0	$P3_0 = A_{3,0} + D_{3,0} + E_{3,0}$
P4	2	1	$P4_1 = A_{4,(2,1)}\cdot C_{4,1}\cdot D_{4,1}\cdot E_{4,2}$
		0	$P4_1 = A_{4,0} + C_{4,0} + D_{4,0} + E_{4,(1,0)}$
P5	3	1	$P5_1 = A_{5,(2,1)}\cdot E_{5,(2,1)}$
		0	$P5_0 = A_{5,0} + E_{5,0}$
P6	3	1	$P6_1 = A_{6,(2,1)}\cdot E_{6,(2,1)}\cdot F_{6,1}$
		0	$P6_0 = A_{6,0} + E_{6,0} + F_{6,0}$

Step 1: construct the MMDD models for each component and states

$A_{1,2} = case(A_1,1,0,0)$ $B_{1,1} = case(B,1,0)$ $C_{1,2} = case(C_1,1,0,0)$

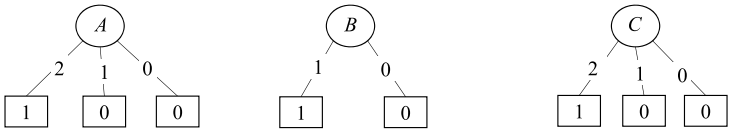

Step 2: integrate the component MMDD models into a system MMDD model steep by step

$A_{1,2} \cdot B_{1,1} = case(A_1,1,0,0) \cdot case(B_1,1,0) = case(A_1, case(B_1,1,0),0,0)$

$A_{1,2} \cdot B_{1,1} \cdot C_{1,2} = case(A_1, case(B_1,1,0),0,0) \cdot case(C_1,1,0,0) = case(A_1, case(B_1, case(C_1,1,0,0),0),0,0)$

Fig. 5. The model construction process of $P1_2$ by the MMDD manipulation rule.

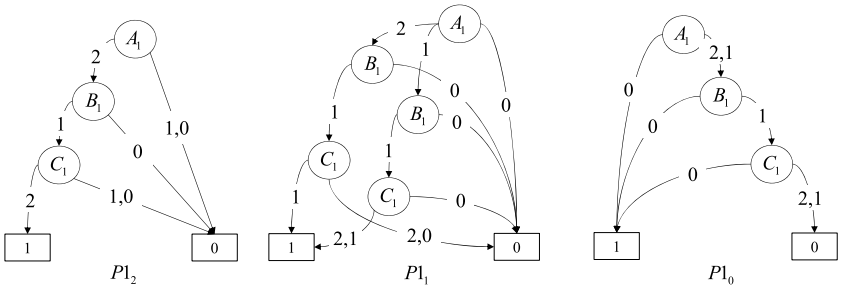

Fig. 6. The MMDD models for $P1_2$, $P1_1$ and $P1_0$.

In this section, Using component E as an example, the model construction process by the backward PDO and forward PDO are both shown in Fig. 8. In Fig. 8, CE_3 and CE_5 represent the behaviors of component E in phase 3 and phase 5, respectively. Furthermore, in Fig. 8, the red numbers are the numbers that changed by different PDOs. For example, $case(E_3,1,0,0)$ in the backward PDO represent that if component E is in state 2 in phase 5, then it must be in state 2 in phase 3. Therefore, the variables representing component E in states 0 and 1 are set be '0'. In Fig. 8, the modeling process by the forward PDO is also shown. In the second line of forward PDO, '$1 \cdot case(E_5,0,1,0)$' represents that component E is in state 1 in phase 3, so it must be in state 1 or 0 in phase 5. As a result, $E_{5,2} = 0$. And '$1 \cdot case(E_5,0,0,0)$' represents that component E is in state 0 in phase 3, so it must be in state 0 in phase 5. As a result, $E_{5,1} = 0, E_{5,2} = 0$.

With the model construction method shown in Fig. 8, the system MMDD model for the mission path η_3^M with the backward PDO and forward PDO are constructed, shown in Fig. 9.And the system MMDD model for mission path η_1^M with backward PDO is also displayed in Fig. 10.

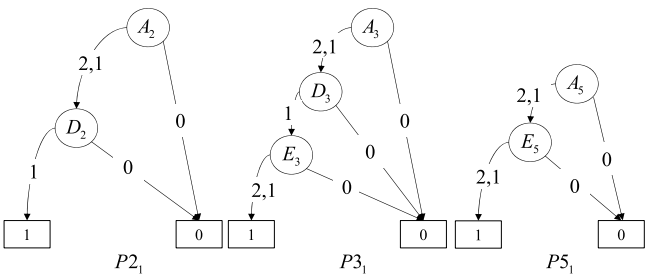

Fig. 7. The MMDD models for phases $P2_1$, $P3_1$ and $P5_1$.

Fig. 9 indicates that the scale of the MMDD model by the backward PDO is smaller than the model by the forward PDO. The main reason is that by the backward PDO, the variables that represent one component in different phases have been integrated into one variable, which could decrease the variable numbers and improve the modeling efficiency. However, it will lead to the unknown passed phases. For example, for the MMDD model with backward PDO, the out-edge '2' of variable E_5 means that component E is still in state 2 at the end of phase 5, and it also represents that component E works in phase 3 and state 2. To represent this difference in these models, the general MMDD manipulation rule shown in Eq. (2) is modified into:

$$G \blacklozenge H = case(A_i,G_m,\cdots,G_1) \blacklozenge case(A_j,H_m,\cdots,H_1) = \begin{cases} case\left(A_i^{ij},G_m \blacklozenge E_{j,1},G_{m-1} \blacklozenge E_{j,2},\cdots,G_2 \blacklozenge E_{j,m-1},G_1 \blacklozenge E_{j,m}\right) \text{Forward PDO} \\ case\left(A_j^{ij},E_{i,m} \blacklozenge H_m,E_{i,m-1} \blacklozenge H_{m-1},\cdots,E_{i,2} \blacklozenge H_1,E_{i,1} \blacklozenge H_1\right) \text{Backward PDO} \end{cases}$$

$$E_{i,n} = case\left(A_i,G_m,\cdots,G_n,\underbrace{0,\cdots,0}_{n-1}\right), E_{j,n} = case\left(A_j,\underbrace{0,\cdots,0}_{n-1},H_{m-n+1},\cdots,H_1\right) \quad (4)$$

In Eq. (4), an extra variable ij is added to A_i. By this way, the variable after manipulated, A_i^{ij} could show the phases that component A has passed. The backward PDO in the MMDD model is applied efficiently in the system modeling of the PMS with dynamic phase selections. And with the improved manipulation rule shown in Eq. (4), the system

Component E works in phases 3 and 5 in the mission path η_3^M

$CE_3 = case(E_3,1,1,0)$ Component E in phase 3

$CE_5 = case(E_5,1,1,0)$ Component E in phase 5

Backward PDO $(E_5 < E_3)$

$$CE_3 \cdot CE_5 = case(E_3,1,1,0)\cdot case(E_5,1,1,0)$$
$$= case\begin{pmatrix} E_5,1\cdot case(E_3,1,0,0),1\cdot case(E_3,1,1,0), \\ 0\cdot case(E_3,1,1,0)\end{pmatrix}$$
$$== case(E_5,1,case(E_3,1,1,0),0)$$

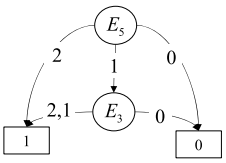

Forward PDO $(E_3 < E_5)$

$$CE_3 \cdot CE_5 = case(E_3,1,1,0)\cdot case(E_5,1,1,0)$$
$$= case\begin{pmatrix} E_3,1\cdot case(E_5,1,1,0),1\cdot case(E_5,0,1,0), \\ 0\cdot case(E_5,0,0,0)\end{pmatrix}$$
$$= case(E_3,case(E_5,1,1,0),case(E_5,0,1,0),0)$$

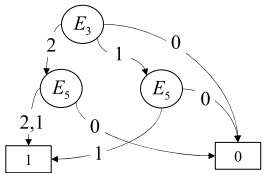

Fig. 8. The backward PDO for component E in the mission path η_3^M.

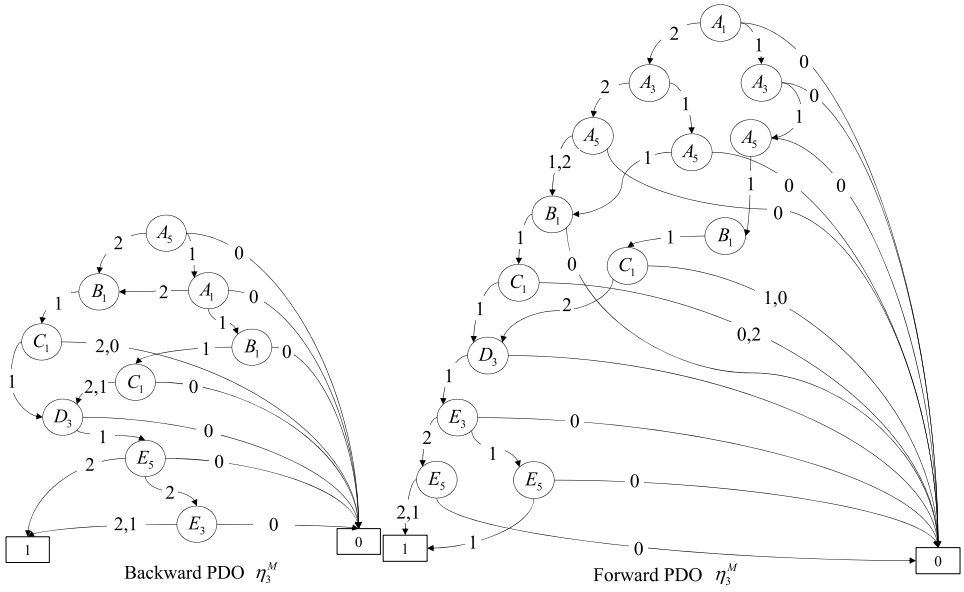

Fig. 9. The MMDD model for mission path η_3^M with backward and forward PDO.

MMDD model for mission path η_3^M is shown in Fig. 11.

In Fig. 11, eight component paths from variable A_5 to '1' by the backward PDO in these two MMDD models. All the component paths leading to the system success is:

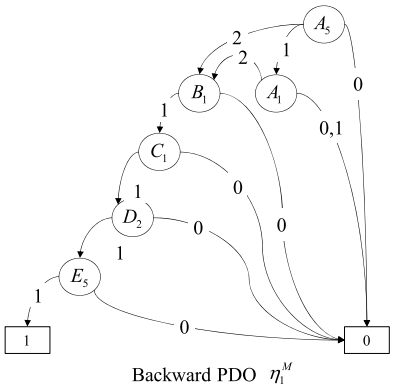

Fig. 10. The MMDD model for mission path η_1^M with backward PDO.

$$\left.\begin{aligned} &\eta_1^C = A_{5,2}^{125}B_{1,1}^1C_{1,1}^1D_{2,1}^2E_{5,(2,1)}^5, \eta_2^C = A_{5,1}^{125}A_{1,2}^1B_{1,1}^1C_{1,1}^1D_{2,1}^2E_{5,(2,1)}^5 \end{aligned}\right\}\eta_1^M$$
$$\left.\begin{aligned} &\eta_3^C = A_{5,2}^{135}B_{1,1}^1C_{1,1}^1D_{3,1}^3E_{5,1}^{35}E_{3,2}^3, \eta_4^C = A_{5,2}^{135}B_{1,1}^1C_{1,1}^1D_{3,1}^3E_{5,2}^{35} \\ &\eta_5^C = A_{5,1}^{135}A_{1,2}^1B_{1,1}^1C_{1,1}^1D_{3,1}^3E_{5,1}^{35}E_{3,2}^3, \eta_6^C = A_{5,1}^{135}A_{1,2}^1B_{1,1}^1C_{1,1}^1D_{3,1}^3E_{5,2}^{35} \\ &\eta_7^C = A_{5,1}^{135}A_{1,2}^1B_{1,1}^1C_{1,2}^1D_{3,1}^3E_{5,1}^{35}E_{3,2}^3, \eta_8^C = A_{5,1}^{135}A_{1,2}^1B_{1,1}^1C_{1,2}^1D_{3,1}^3E_{5,2}^{35} \end{aligned}\right\}\eta_3^M \quad (5)$$

In Eq. (5), $A_{5,2}^{135}$ represents that component A is in state 2 at the end of phase 5 and it works in phase 1, 3, and 5 in this component path. With the component paths shown in Eq. (5), the system probability leading to mission success could be evaluated.

3.3. Modeling validation and modeling efficiency comparison

(1) Model construction efficiency comparison

In this section, using mission η_3^M as an example, the modeling efficiencies with multiple phases and components by the improved backward PDO and forward PDO are studied.

Firstly, the modeling efficiencies with increasing phase numbers are

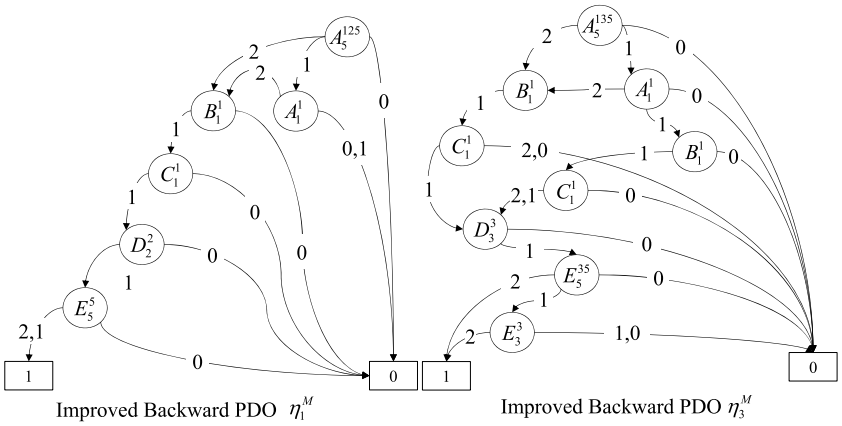

Fig. 11. The MMDD models for paths η_1^M and η_3^M with improved backward PDO.

Table 3
The modeling efficiency with different phase numbers.

	Phased number	5	6	7	8	9	10	11	12
Proposed method	Time (s)	0.0172	0.0226	0.0330	0.0392	0.0492	0.0714	0.0921	0.1247
	number of calls	234	324	430	575	781	1045	1421	1821
Forward PDO	Time (s)	0.0205	0.0513	0.1129	0.3156	0.5023	1.0234	3.5132	14.6129
	number of calls	289	813	1746	4732	6827	14270	40291	120457

Table 4
The modeling efficiency with different component numbers.

Component number		5	6	7	8	9	10	11	12
Proposed method	Time (s)	0.0175	0.0182	0.0232	0.0321	0.0367	0.0432	0.0634	0.0805
	number of calls	240	287	339	415	532	703	912	1142
Forward PDO	Time (s)	0.0179	0.0429	0.0903	0.295	0.4331	0.9060	2.7135	12.6129
	number of calls	299	713	1592	4437	6174	12649	34228	93913

shown in Table 3, with the forward PDO and improved backward PDO-based algorithms. In the modeling, the phases in the path η_3^M are recurring. For example, when the phase number is 5, the constructed model is $\eta^M = P1_1P3_1P5_1P1_1P3_1$.

Secondly, the modeling time with increasing component numbers is shown in Table 4. As shown in Fig. 11, there are five components in the mission path η_3^M. All the increased components are connected to the components in parallel from component A~ component E. Then, the modeling efficiencies with different nuber of compoents are shown in Table 4.

From the comparison in Table 3 and Table 4, the modeling efficiency of the proposed method is much better than the forward PDO-based method, especially for large-scale PMSs.

(2) Compared to BDD based method

In this section, the proposed MMDD-based method is compared to the PMS-BDD-based method [7] to show the correctness and effectiveness of the proposed method. The modeling process of the PMS-BDD model is shown in Fig. 12.

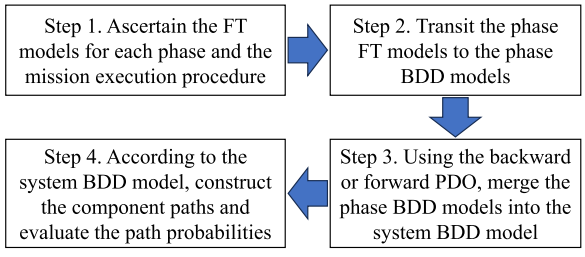

Fig. 12. The system modeling process of PMS-BDD based model.

The system BDD model for mission paths η_3^M and η_1^M are shown in Fig. 13. One can see that the model scale of the MMDD models is less than the BDD model (η_1^M 6 nodes *vs* 8 nodes, η_3^M 9 nodes *vs* 14 nodes). The reason is that for the multistate components, one variable is enough to represent the multi-state behaviors. However, multiple variables are necessary to represent multi-state behaviors. And with more components' states, more variables are needed in the BDD models.

Secondly, according to the models shown in Fig. 13, the component paths for mission path η_1^M could be evaluated as:

$$\left.\begin{array}{l}\eta_1^C = A_{5,2}^{135}B_{1,1}^1C_{1,1}^1D_{3,1}^3E_{5,1}^{35}E_{3,2}^3, \eta_2^C = A_{5,2}^{135}B_{1,1}^1C_{1,1}^1D_{3,1}^3E_{5,2}^{35} \\ \eta_3^C = A_{5,1}^{135}A_{1,2}^1B_{1,1}^1C_{1,1}^1D_{3,1}^3E_{5,1}^{35}E_{3,2}^3, \eta_4^C = A_{5,1}^{135}A_{1,2}^1B_{1,1}^1C_{1,1}^1D_{3,1}^3E_{5,2}^{35} \\ \eta_5^C = A_{5,1}^{135}A_{1,2}^1B_{1,1}^1C_{1,2}^1D_{3,1}^3E_{5,1}^{35}E_{3,2}^3, \eta_6^C = A_{5,1}^{135}A_{1,2}^1B_{1,1}^1C_{1,2}^1D_{3,1}^3E_{5,2}^{35}\end{array}\right\}\eta_3^M$$
$$\left.\eta_7^C = A_{5,2}^{125}B_{1,1}^1C_{1,1}^1D_{2,1}^2E_{5,(2,1)}^5, \eta_8^C = A_{5,2}^{125}A_{1,2}^1B_{1,1}^1C_{1,1}^1D_{2,1}^2E_{5,(2,1)}^5\right\}\eta_1^M \quad (6)$$

Compared the component paths shown in Eqs. (5) and (6), we can see that they are matched. This comparison shows the modeling efficiency and correction of the proposed model construction mechanism.

4. Probability evaluation method

In this section, the probabilities of all paths will be evaluated by the proposed Markov renewal equation-based method, considering two key factors, random phase durations and non-exponential state transition distributions. These two factors are common in practical engineering and ignored in most of the PMS reliability analysis methods. As shown in Fig. 14, the state transition time could follow any distribution, $F_{i,j}(t)$. As

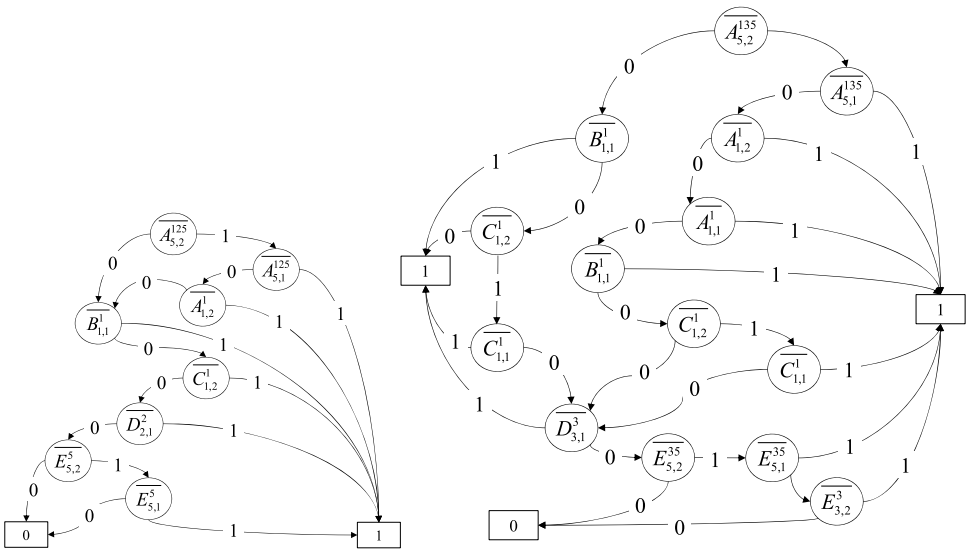

Fig. 13. The system BDD models for mission paths η_1^M and η_3^M.

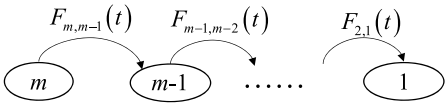

Fig. 14. The state transition diagram of a multistate component without repair.

a result, the traditional Markov chain is not available. To this end, an improved Markov-renewal equation-based method is proposed in this section.

4.1. Markov renewal theory

Fig. 14 indicates that the state transition time between states does not follow the exponential distribution, which means the memoryless property does not exist during the state transitions. Therefore, the Markov renewal equation-based method is applied to evaluate the state probabilities. To evaluate the system state probabilities, two matrices, $\boldsymbol{Q}(t)$ and $\boldsymbol{\theta}(t)$, which are the kernel matrix and state transition probability matrix, are used in this article. Each element, $Q_{i,j}(t)$, in the kernel matrix $\boldsymbol{Q}(t)$, represents the process transit from state i to state j in once transition. In general, $Q_{i,j}(t)$ could be evaluated by the competing failure behaviors. In this article, all the components are degraded linearly, and the states can only change into the adjacent state, therefore, $Q_{i,j}(t)$ is equal to $F_{i,j}(t)$.

Then, the elements, $\theta_{i,j}(t)$ in $\boldsymbol{\theta}(t)$, represents the transition probability of the process from state i to state j with multiple steps. And with matrix $\boldsymbol{Q}(t)$, $\boldsymbol{\theta}(t)$ could be evaluated by the Markov renewal equation, as:

$$\theta_{i,j}(t) = \begin{cases} 1 - \sum_{j=1(j\neq i)}^{m} Q_{i,j}(t), i = j \\ \sum_{k=1}^{m} \int_0^t q_{i,k}(\tau)\theta_{k,j}(t-\tau)d\tau, i \neq j \end{cases} \tag{7}$$

$$q_{i,k}(t) = dQ_{i,j}(t)/dt$$

With the evaluated system state transition probability matrix $\boldsymbol{\theta}(t)$, the state probabilities at any time could be evaluated with the initial state probability, as:

$$\boldsymbol{P}(t) = \boldsymbol{P}(0)\boldsymbol{\theta}(t) \tag{8}$$

4.2. Path evaluation method

Components are assumed to be independent on each other. Therefore, the path probability could be evaluated by multiplying the probabilities of each component with different states in different phases. For example, the probability of the path η_5^C shown in Eq. (5) could be evaluated as:

$$\begin{aligned} \Pr(\eta_5^C) &= \Pr\left(A_{5,1}^{135}A_{1,2}^{1}B_{1,1}^{1}C_{1,1}^{1}D_{3,1}^{3}E_{5,1}^{35}E_{3,2}^{3}\right) \\ &= \Pr\left(A_{5,1}^{135}A_{1,2}^{1}\right)\Pr\left(B_{1,1}^{1}\right)\Pr\left(C_{1,1}^{1}\right)\Pr\left(D_{3,1}^{3}\right)\Pr\left(E_{5,1}^{35}E_{3,2}^{3}\right) \end{aligned} \tag{9}$$

In Eq. (9), $A_{5,1}^{135}A_{1,2}^{1}$ represents component A works in phases 1, 3 and 5. Meanwhile, the component state is in state 2 at the end of phase 1. Then, it degrades into state 1 at the end of phase 3 and it stays in state 1 until the end of phase 5. In this article, there are two difficulties in the path probability evaluation: (i) The non-exponential multistate component does not possess the memoryless property during component state transitions, which made the components' state transition behaviors

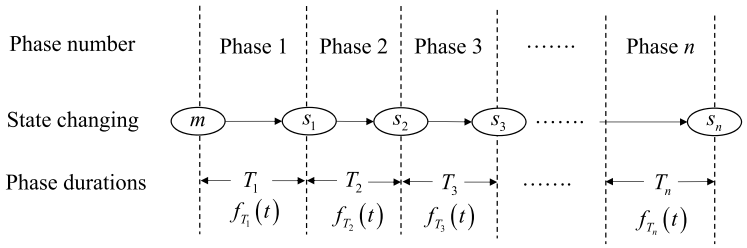

Fig. 15. The state transition paths of component A in multiple phases.

among phases are connected. (ii) The phase durations follow different distributions.

With random phase durations and non-exponential state transition distributions, the component state transition behaviors will be very complex. To show the state probability evaluation method, a component A with m states and n phases is used to show the proposed method. Assuming that component A is in state m at the beginning of phase 1 and the component state at the end of each phase is denoted as $s_1, s_2, s_3, \ldots, s_n$ ($m > s_1 > s_2 > s_3 > \cdots > s_n$), respectively. And the phase durations also follow different distributions $T_i \sim f_{T_i}(t)$. The state transition paths this state combinations is shown in Fig. 15.

According to Fig. 15, the probability that the state of component A transition in this path could be evaluated as:

$$\begin{aligned}
&\Pr(S_0 = m, S_{T_1} = s_1, S_{T_2} = s_2, S_{T3} = s_3, \cdots, S_{T_n} = s_n) \\
&= \int_0^{+\infty} \cdot \int_0^{T-t_1-t_2-\cdots-t_{n-1}} \left[\begin{array}{l} \int_0^{t_1} f_{m,s_1}(\tau_1) \int_0^{t_2} f_{s_2,s_1}(\tau_2 + T_1 - \tau_1) \int_0^{t_3} f_{s_2,s_3}(\tau_3 + T_2 - \tau_2) \cdots \\ \int_0^{t_n} \sum_{k=s_{n-1}}^{s_n} f_{s_{n-1},k}(T_n + \tau_n - \tau_{n-1}) \theta_{k,s_n}(T_n - \tau_n) d\tau_n \cdots d\tau_1 \end{array} \right] \\
&\quad f_{T_1}(t_1) \cdots f_{T_n}(t_n) dt_1 \cdots dt_n
\end{aligned}$$

Proof.

Firstly, consider two simple cases, the state transition probability evaluation with one phase and two-phase cases.

For a one phase case, the component transit from state m to state s_1 and the phase duration follows a normal distribution $T_1 \sim f_{T_1}(t)$. Then, the probability could be evaluated as:

$$\begin{aligned}
\Pr(S_0 = m, S_{T_1} = s_1) &= \Pr\{Z(T_1) = s_1, T_1 | Z(0) = m\} \\
&= \int_0^{+\infty} \Pr(Z(T_1) = s_1, T_1 = t_1 | Z(0) = m) dt_1 \\
&= \int_0^{+\infty} \sum_{k=s_1}^{m} \int_0^{t_1} f_{m,k}(\tau) \theta_{k,s_1}(t - \tau) d\tau f_{T_1}(t_1) dt_1
\end{aligned} \tag{10}$$

$$\begin{aligned}
&\Pr(S_0 = m, S_{T_1} = s_1, S_{T_2} = s_2) \\
&= \Pr\{Z(t_1) = s_1, Z(T_2) = s_2, T_1 = t_1, T_2 = t_2 | Z(0) = m\} \\
&= \int_0^{+\infty} \int_0^{T-t_2} \Pr(Z(T) = s_1, Z(T_2) = s_2 | Z(0) = m) f_{T_1}(t_1) f_{T_2}(t_2) dt_1 dt_2 \\
&= \int_0^{+\infty} \int_0^{T-t_2} \left[\int_0^{t_1} f_{m,s_1}(\tau_1) \int_0^{t_2} \sum_{k=s_1}^{s_2} f_{s_1,k}(\tau_2 + T_1 - \tau_1) \theta_{k,s_2}(T_2 - \tau_2) \, d\tau_2 d\tau_1 \right] f_{T_1}(t_1) f_{T_2}(t_2) dt_1 dt_2
\end{aligned} \tag{11}$$

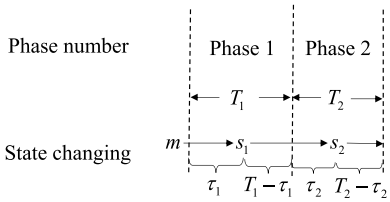

Fig. 16. The state transition paths of component A in 2 phases.

In Eq. (10), $f_{m,k}(\tau)$ represents the state transition probability of component A from state m to state k and if $k - m = 1$, $f_{m,k}(\tau) = q_{m,k}(\tau)$. And if $k - m > 1$, $f_{m,k}(\tau) = \sum_{s=m+1}^{k} q_{m,s}(\tau) q_{s,k}(\tau)$, which means that each transition possibility from state m to state k is taken into consideration. For a two-phase case, the state transition process is more complicated. The state transitions are shown in Fig. 16. In this transition process, the known condition is that the component state at the beginning, the end of phase 1 and the end of phase 2 are m, s_1 and s_2, respectively. Assuming the precise transit timing is τ_1 and τ_2, we can know that component A transit from state m to state s_1 during time interval $[0, \tau_1]$, then transit from state s_1 to state s_2 during time interval $[\tau_1, \tau_2]$. τ_1 and τ_2 could be any values between time intervals $[0, T_1]$ and $[0, T_2]$, respectively.

According to the description, the probability could be evaluated as:

Then, by analogy, for an n-phases case, if the component state at the end of each phase is s_1, s_2, …, s_n ($m>s_1>s_2>\ldots>s_n$), the probability could be evaluated as:

$$\begin{aligned}&\Pr(S_0=m,S_{T_1}=s_1,S_{T_2}=s_2,S_{T3}=s_3,\cdots,S_{T_n}=s_n)\\&=\int_0^{+\infty}\cdot\int_0^{T-t_1-t_2-\cdots-t_{n-1}}\left[\begin{array}{l}\int_0^{t_1}f_{m,s_1}(\tau_1)\int_0^{t_2}f_{s_1,s_2}(\tau_2+T_1-\tau_1)\int_0^{t_3}f_{s_2,s_3}(\tau_3+T_2-\tau_2)\cdots\\\int_0^{t_n}\sum_{k=s_{n-1}}^{s_n}f_{s_{n-1},k}(T_n+\tau_n-\tau_{n-1})\theta_{k,s_n}(T_n-\tau_n)d\tau_n\cdots d\tau_1\end{array}\right]\\&\quad f_{T_1}(t_1)\cdots f_{T_n}(t_n)dt_1\cdots dt_n\end{aligned}\tag{12}$$

Consider a special case in which the component state is not changing during one phase, which means that the component state does not change during this time duration. The state transition does not occur during this time duration. Then, the evaluation could be simplified. For example, if $s_2=s_1$ in Eq. (12). The probability is:

$$\begin{aligned}&\Pr(S_0=m,S_{T_1}=s_1,S_{T_2}=s_2,S_{T3}=s_3,\cdots,S_{T_n}=s_n)\\&=\int_0^{+\infty}\cdot\int_0^{T-t_1-t_2-\cdots-t_{n-1}}\left[\begin{array}{l}\int_0^{t_1}f_{m,s_1}(\tau_1)\int_0^{t_3}f_{s_1,s_3}(\tau_3+T_2+T_1-\tau_1)\cdots\\\int_0^{t_n}\sum_{k=s_{n-1}}^{s_n}f_{s_{n-1},k}(T_n+\tau_n-\tau_{n-1})\theta_{k,s_n}(T_n-\tau_n)d\tau_n\cdots d\tau_1\end{array}\right]\\&\quad f_{T_1}(t_1)\cdots f_{T_n}(t_n)dt_1\cdots dt_n\end{aligned}\tag{13}$$

With Eqs. (12) and (13), the component path probability could be evaluated. However, we can see that the multi-integrals in these functions are very complex. And with non-exponential distributions, i.e., the Weibull distribution, it's very complex to evaluate an analytical solution for these complicated multi-integrals. Therefore, an approximation algorithm, the trapezoidal integration method, is applied. By this method, a high-precision approximate solution could be computed.

In the following, two special cases, exponential multistate components, and fixed phase durations, which are commonly seen in previous research, are also given.

(1) Exponential multistate components [32]

If the state transition time of each component follows the exponential distribution, the memoryless property is possessed at any time. All the components' memory will be lost after the phase change. For example, in Fig. 16, the component state transition rate at time τ_1 and T_1 is the same. So the path probability evaluation equation shown in Eq. (12) could be simplified as:

Table 5
Component parameters for the AOCS.

Components	parameters	Components	parameters
A	$\alpha_{2,1}=1.8,\beta_{2,1}=1500h^{-1}$ $\alpha_{1,0}=2.5,\beta_{1,0}=1200h^{-1}$	F	$\alpha_{2,1}=1.5,\beta_{2,1}=2500h^{-1}$ $\alpha_{2,1}=2,\beta_{2,1}=1800h^{-1}$
B	$\alpha_{1,0}=1.3,\beta_{1,0}=5500h^{-1}$	G	$\alpha_{2,1}=1.5,\beta_{2,1}=2500h^{-1}$
C	$\alpha_{1,0}=1.3,\beta_{1,0}=4000h^{-1}$	H	$\alpha_{1,0}=1.3,\beta_{1,0}=6000h^{-1}$
D	$\alpha_{1,0}=1.3,\beta_{1,0}=8000h^{-1}$		$\alpha_{1,0}=1.4,\beta_{1,0}=5000h^{-1}$
E	$\alpha_{1,0}=1.3,\beta_{1,0}=6000h^{-1}$		

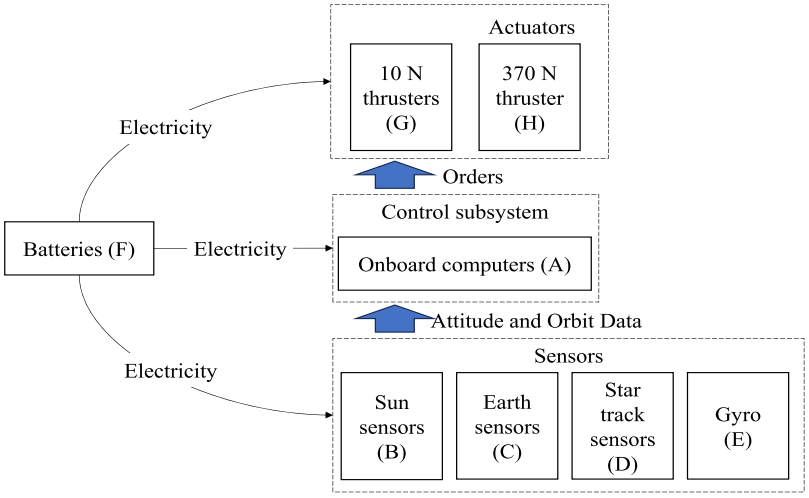

Fig. 17. The consisting components of the AOCS.

$$\Pr(S_0 = m, S_{T_1} = s_1, S_{T_2} = s_2, S_{T3} = s_3, \cdots, S_{T_n} = s_n) = \int_0^{+\infty} \cdot \int_0^{T-t_1-t_2-\cdots-t_{n-1}} \left[\begin{array}{l} \int_0^{t_1} f_{m,s_1}(\tau_1) \int_0^{t_2} f_{s_1,s_2}(\tau_2) \int_0^{t_3} f_{s_2,s_3}(\tau_3)\cdots \\ \int_0^{t_n} \sum_{k=s_{n-1}}^{s_n} f_{s_{n-1},k}(\tau_n)\theta_{k,s_n}(\tau_n) d\tau_n \cdots d\tau_1 \end{array} \right] f_{T_1}(t_1)\cdots f_{T_n}(t_n) dt_1 \cdots dt_n \tag{14}$$

(2) Fixed phase durations [25]

Another special situation is the fixed phase durations. If the phase durations are fixed, that T_1, T_2,..., T_n are fixed, the path probability evaluation equation shown in Eq. (12) could be simplified as:

$$\begin{aligned} &\Pr(S_0 = m, S_{T_1} = s_1, S_{T_2} = s_2, S_{T3} = s_3, \cdots, S_{T_n} = s_n) \\ &= \int_0^{T_1} f_{m,s_1}(\tau_1) \int_0^{T_2} f_{s_1,s_2}(\tau_2 + T_1 - \tau_1) \int_0^{T_3} f_{s_2,s_3}(\tau_3 + T_2 - \tau_2)\cdots \\ &\quad \int_0^{T_n} \sum_{k=s_{n-1}}^{s_n} f_{s_{n-1},k}(T_n + \tau_n - \tau_{n-1})\theta_{k,s_n}(T_n - \tau_n) d\tau_n \cdots d\tau_1 \end{aligned} \tag{15}$$

5. Illustrations

5.1. Description

The Attitude and Orbit Control System (AOCS) in a spacecraft is used to show the proposed method's capability. The AOCS is used to control the attitude and orbit during the whole lifetime, which is critical for the spacecraft. The AOCS consists of several functional subsystems, control subsystem (A), different kinds of sensors (B, C, D, E), batteries (F), and actuators (G, H), as shown in Fig. 17. Component A, Fand H have three states and all the sensors have two states. All the parameters for the components are shown in Table 5. The components' state transition time follows the Weibull distribution, and $\alpha_{i,j}$ and $\beta_{i,j}$ are the shape parameters and scale parameters, respectively. All these data listed here have been decrypted.

The whole mission process could be divided into several missions and phases. During the whole lifetime, there are four missions (launching, orbit transfer, on-orbit operation and back to earth) need to be completed in different phases, as shown in Fig. 18. During the whole lifetime, the control subsystem, component A, needs to be in a different working state. Then, in phase 1, components C and F are used to acquire the attitude data and provide electricity. In phase 2, the earth sensor and sun sensors are combined to work. If they are working normally until the next phase, the system will execute phase 3 to finish mission 3. And if any of them fail, the star track sensors and gyro will be used in phase 4 as an alternative to finish the following missions. At last, the star track sensors and gyro will be used in phase 5 to finish the last mission. In addition, the 10 N thrusters and 370N thruster will be used in P2/P5 and P3/P4 for orbit maintenance and orbit transfer, respectively. And the system structure functions and time durations for different phases are also shown in Table 6. All the phase durations follow different distributions. For example, T_1 and T_2 follow the uniform distribution and normal distribution, respectively.

5.2. System reliability

According to the model construction procedure shown in Section 3, the system reliability of the AOCS could be evaluated, as shown in the following.

Step 1. Construct the mission paths for the whole system:

$$\begin{aligned} \eta_1^M &= P1_1P2_2P3_1P5_1 \\ \eta_2^M &= P1_1P2_1P4_1P5_1 \end{aligned} \tag{16}$$

According to the mission paths, construct the MMDD models for different phases and states, as shown in Fig. 19.

Step 2. According to the improved MMDD manipulation rule shown in Eq. (4), construct the system MMDD models for different mission paths in Eq. (16).

Step 3. According the MMDD models shown in Fig. 20, the component paths for the whole system successing could be evaluated. There are 8 paths for the mission path η_1^m:

$$\left.\begin{aligned} \eta_1^C &= A_{5,2}^{1235}B_{3,1}^{23}C_{3,1}^{123}D_{5,1}^{5}E_{5,1}^{5}F_{2,2}^{12}H_{5,2}^{25}, \\ \eta_2^C &= A_{5,1}^{1235}A_{5,2}^{12}B_{3,1}^{23}C_{3,1}^{123}D_{5,1}^{5}E_{5,1}^{5}F_{2,2}^{12}H_{5,2}^{25} \\ \eta_3^C &= A_{5,2}^{1235}B_{3,1}^{23}C_{3,1}^{123}D_{5,1}^{5}E_{5,1}^{5}F_{2,1}^{12}F_{2,2}^{1}H_{5,2}^{25}, \\ \eta_4^C &= A_{5,1}^{1235}A_{5,2}^{12}B_{3,1}^{23}C_{3,1}^{123}D_{5,1}^{5}E_{5,1}^{5}F_{2,1}^{12}F_{2,2}^{1}H_{5,2}^{25} \\ \eta_5^C &= A_{5,2}^{1235}B_{3,1}^{23}C_{3,1}^{123}D_{5,1}^{5}E_{5,1}^{5}F_{2,2}^{12}H_{5,1}^{25}H_{2,2}^{22}, \\ \eta_6^C &= A_{5,1}^{1235}A_{5,2}^{12}B_{3,1}^{23}C_{3,1}^{123}D_{5,1}^{5}E_{5,1}^{5}F_{2,2}^{12}H_{5,1}^{25}H_{2,2}^{22} \\ \eta_7^C &= A_{5,2}^{1235}B_{3,1}^{23}C_{3,1}^{123}D_{5,1}^{5}E_{5,1}^{5}F_{2,1}^{12}F_{2,2}^{1}H_{5,1}^{25}H_{2,2}^{22}, \\ \eta_8^C &= A_{5,1}^{1235}A_{5,2}^{12}B_{3,1}^{23}C_{3,1}^{123}D_{5,1}^{5}E_{5,1}^{5}F_{2,1}^{12}F_{2,2}^{1}H_{5,1}^{25}H_{2,2}^{22} \end{aligned}\right\} \eta_1^M \tag{17}$$

For mission path η_2^m, there are 16 paths shown as:

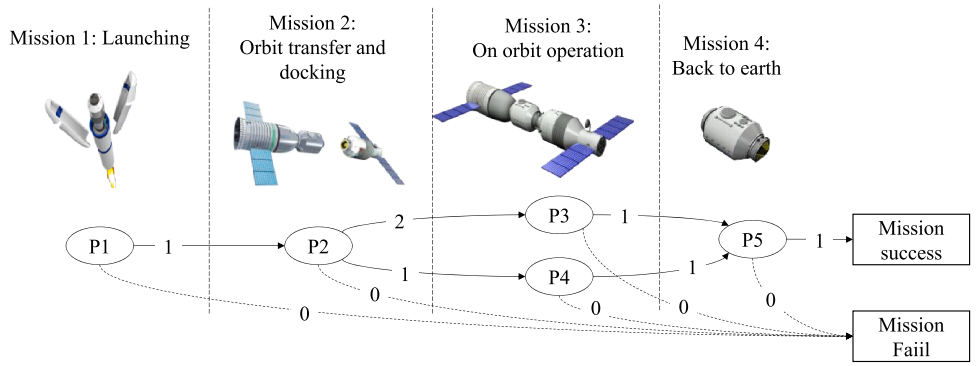

Fig. 18. The missions and phases of the AOCS.

Table 6
System structure functions and durations for different phases of the AOCS.

Phases	States	System structures	Phase durations (h)
P1	1	$P1_1 = A_2C_1F_2$	$T_1 \sim U(18,22)$
P2	2	$P2_2 = A_2B_1C_1F_2H_1$	$T_2 \sim N(24,5.2)$
	1	$P2_1 = A_2B_0C_1F_2H_2 + A_2B_1C_0F_2H_2 + A_2B_0C_0F_2H_2$	
P3	1	$P3_1 = A_{(2,1)}B_1C_1G_1$	$T_3 \sim N(120,6.1)$
P4	1	$P4_1 = A_{(2,1)}D_1E_1G_1$	$T_4 \sim N(144,4.8)$
P5	1	$P5_1 = A_{(2,1)}D_1E_1H_{(2,1)}$	$T_5 \sim U(24,36)$

$$\left.\begin{aligned} &\eta_9^C = A_{5,2}^{1245}B_{2,0}^{2}C_{3,1}^{123}D_{5,1}^{45}E_{5,1}^{45}G_{4,1}^{4}F_{2,2}^{12}H_{5,2}^{25}, \\ &\vdots \\ &\eta_{24}^C = A_{5,1}^{1245}A_{2,2}^{12}B_{2,1}^{2}C_{2,1}^{12}D_{5,1}^{45}E_{5,1}^{45}F_{2,1}^{12}F_{1,2}^{1}G_{4,1}^{4}H_{5,1}^{25}H_{2,2}^{2} \end{aligned}\right\} \eta_2^M \tag{18}$$

Step 4. According to the component paths shown in Eq. (18), the system reliability could be evaluated with the path probability evaluation method in Section 4. The system reliability could be evaluated by adding all the probabilities of paths leading to success. The evaluated system reliability with the proposed method is 0.9563595.

5.3. Validation and comparison

5.3.1. Validation by MC simulation method

In this section, the evaluated system reliability of the AOCS is compared to the MC simulation-based method for verification. As we all know, the MC simulation is based on random simulation and statistical analysis. The MC simulations are particularly useful in situations where analytical solutions are difficult or impossible to obtain. And the evaluated result by the MC simulation could be more accurate with more simulations.

Firstly, the simulation procedure for the paths is shown in Fig. 21. Using the component paths η_1^C and η_2^C in Eq. (17) as examples, the path probabilities of these two component paths are evaluated by the proposed method and MC simulation method with different simulation amounts. The simulations are carried out with different simulation amounts 30 times. The comparison results of the two paths are shown in Fig. 22 and Table 7.

Fig. 22 and Table 7 indicate that with the increasing of simulation amount, the errors between the two methods are smaller and smaller. Therefore, we can have a conclusion that the proposed method could provide a highly precise approximation result. Secondly, with the same computer, the evaluation time of the proposed method (segmentation $\delta = 0.1$) is only 2.52397 s. Therefore, the proposed method is more efficient.

From the equations shown in Section 4.2, it can be easily seen that the multiple integrals are very complex, and a numerical integration-based method is used to evaluate the path probabilities. In this section, the evaluation efficiency and accuracy of this method are shown. Using paths η_1^C and η_2^C as examples, and the standard is the evaluated result shown in Section 5.2, the comparison result with different segmentation δ is shown in Table 8.

From Table 8, we can see that with the increase of δ, the computation time, as well as the errors, are also increased. Compared to the results shown in Table 7, the evaluation efficiency of the proposed method is much higher.

5.3.2. Sensitivity analysis

In this section, a sensitivity analysis is carried out to show which component has a greater influence on the system reliability. The state transition probabilities of all components follow the Weibull distribution, in which the scale parameters are directly related to the components' lifetime. Therefore, the sensitivity analysis on the parameter β is carried out. When the parameter β of different components changes from 0.5β to 1.5β, the system reliability changes are shown in Fig. 23.

From Fig. 23, we can see that component A has the greatest influence

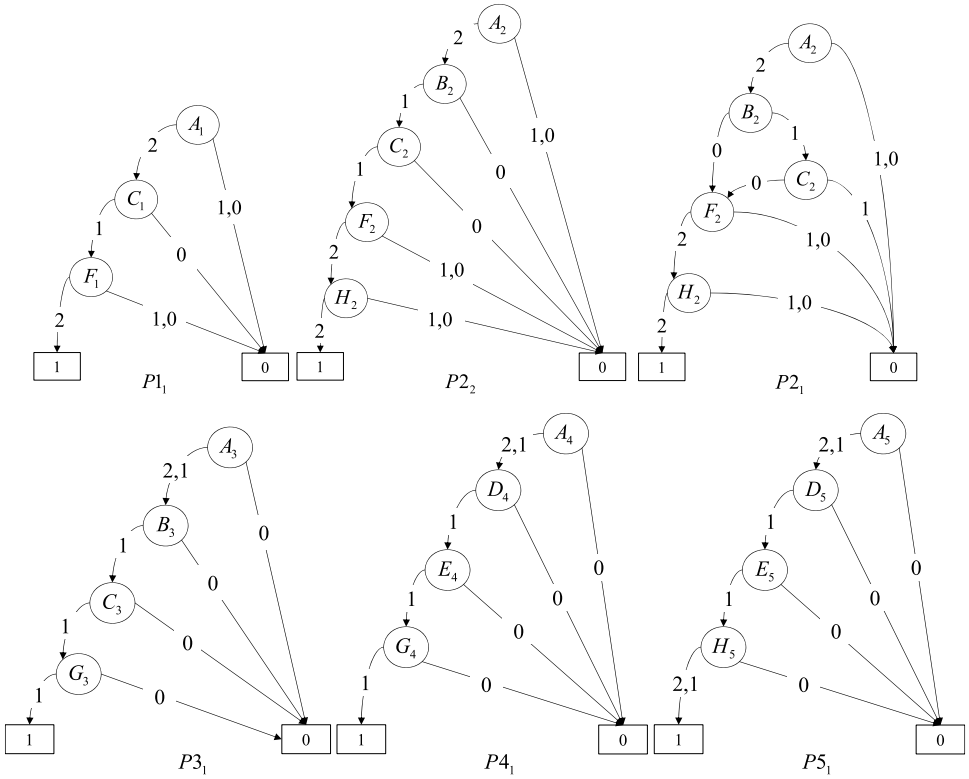

Fig. 19. The MMDD models for different phases of the AOCS.

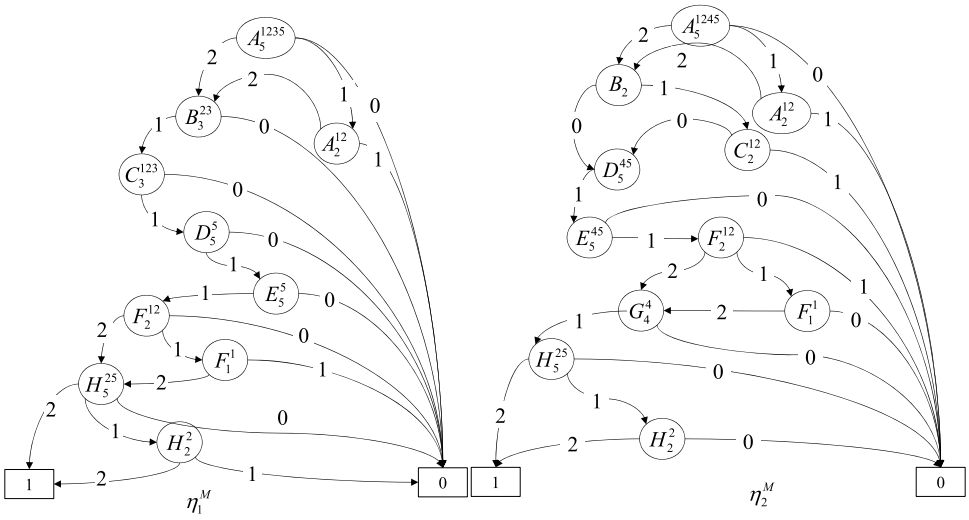

Fig. 20. The MMDD models for different mission paths of the AOCS.

on the system reliability. The reason is that component A works in all phases and the lifetime of component A is also small due to the small β. On the other hand, we can see that both components D, E and F have little influence on the system reliability. For component F, it only works in phase 1 and phase 2, whose durations are very small. And for components D and E, they work in phases 4 and 5. Phase 4 is a backup phase and the duration of phase 5 is also very small. Therefore, the parameter changing of components D, E and F have a small impact on the system reliability.

5.3.3. Comparison

In Ref. [34], the system reliability of PMS with random phase durations and non-exponential components is studied and a Markov regenerative process-based method is proposed for system reliability evaluation. However, an assumption is made that the memory is losable, only during the phase change. By this assumption, the component state is new at the beginning of each phase. With this assumption, the path evaluation function shown in Eq. (12) could be simplified as:

$$\begin{aligned}&\Pr(S_0 = m, S_{T_1} = s_1, S_{T_2} = s_2, S_{T3} = s_3, \cdots, S_{T_n} = s_n)\\ &= \int_0^{+\infty} \cdot \int_0^{T-t_1-t_2-\cdots-t_{n-1}} \theta_{m,s_1}(t_1) f_{T_1}(t_1) \theta_{s_1,s_2}(t_2) f_{T_2}(t_2) \cdots \theta_{s_{n-1},s_n}(t_n) f_{T_n}(t_n) dt_1 \cdots dt_n\end{aligned} \tag{19}$$

With the evaluation function shown in Eq. (19), the path probabilities of path η_1^C and η_2^C could also be evaluated. the comparisons of the proposed method, MC simulation method with simulation amount 2×10^6 [1] and the method in Ref [34] are shown in Table 9.

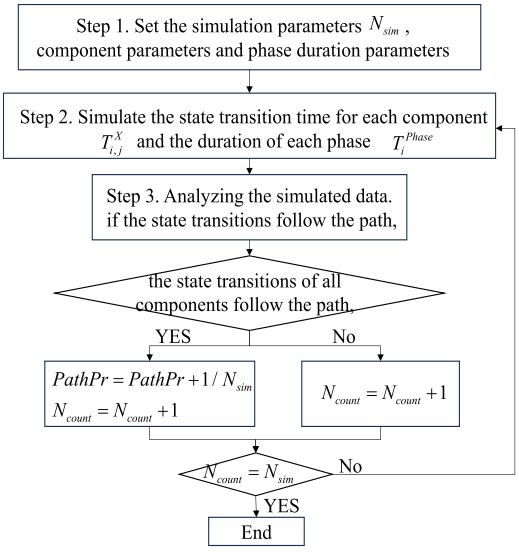

Fig. 21. The Monte Carlo simulation procedure.

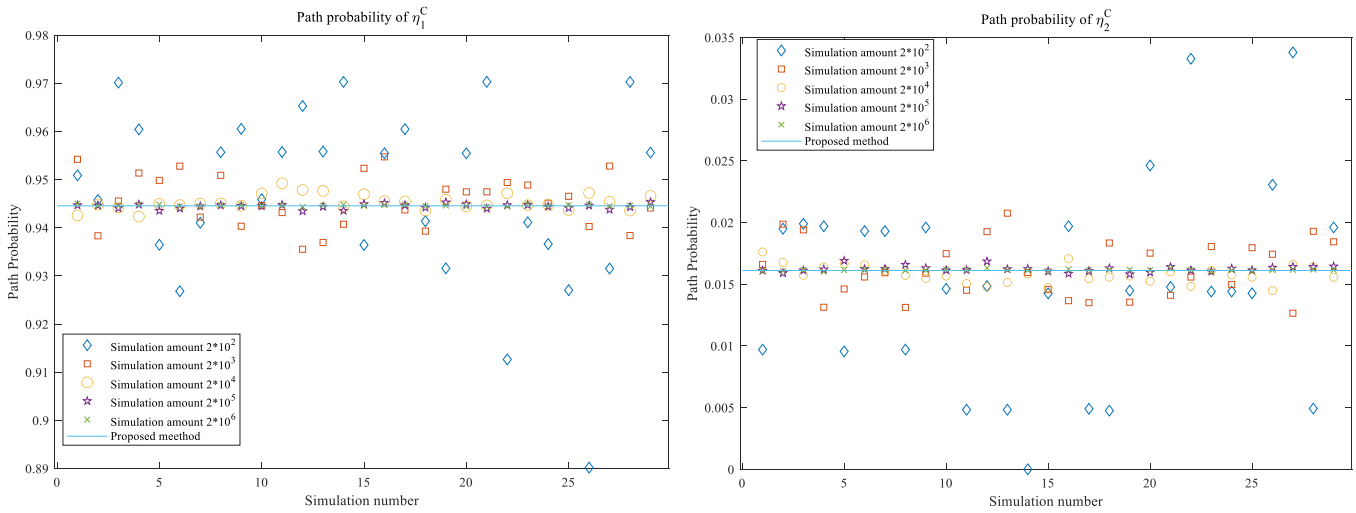

Fig. 22. The path probabilities comparison between proposed and MC simulation methods.

Table 7
The evaluation results by the MC simulation with different amount.

	Simulations	2×10^2	2×10^3	2×10^4	2×10^5	2×10^6
Path η_1^C	Mean values	0.931494	0.950694	0.947294	0.945619	0.944602
	Mean Errors	0.0145	0.0047	0.0013	3.75×10^{-4}	1.39×10^{-4}
	Time (s)	0.82	8.5	79.2	823.3	7823.1
Path η_2^C	Mean values	0.017145	0.016625	0.016285	0.016070	0.016178
	Mean Errors	9.900×10^{-4}	4.470×10^{-4}	1.301×10^{-4}	8.602×10^{-5}	2.032×10^{-5}
	Time (s)	0.76	7.4	81.2	793.4	7958.6

Table 8
Result analysis of proposed method with different segmentation δ.

	δ	0.5	0.4	0.3	0.2	0.1
Path η_1^C	Value	0.930837	0.938149	0.943912	0.945434	0.945994
	Error	0.0152	0.0078	0.0021	0.00056	0
	Time (s)	0.01239	0.02593	0.03125	0.24352	2.52391
Path η_2^C	Value	0.014516	0.015416	0.015743	0.016014	0.016155
	Error	1.639×10^{-3}	7.392×10^{-4}	4.120×10^{-4}	1.410×10^{-4}	0
	Time (s)	0.01066	0.02515	0.04116	0.315662	2.77336

Table 9 confirms that for path η_1^C, the results by the proposed method and the method in Ref. [34] are the same. The reason is that in path η_1^C, the states of all the components are the same at the beginning and the end. And in path η_2^C, the state of component A transits from state 2 to state 1 in phase 3. We can see that the probability of the proposed method is lower. The reason is that in Ref. [34], due to the memoryless assumption, after phase change, the state residence time is set to be zero. However, it should be $\tau(\tau$ could be any value during $[T_1+T_2, T_1+T_2+T_3])$, which leads to a higher state transition rate from state 1 to state 0 in phase 5. By considering this characteristic, the evaluated path probability by the proposed method is lower, and precisely.

6. Conclusions

In this study, tailored to address practical engineering scenarios, novel reliability modeling methodologies are proposed for multistate-phased mission systems (MS-PMS) characterized by random phase durations and dynamic phase combinations. Initially, a multi-state multi-valued decision diagram-based (MMDD-based) modeling approach is introduced to accommodate dynamic phase combinations, wherein phase selection is contingent upon the system state of the preceding phase. Comparative analyses are conducted with the PMS-MMDD model featuring forward-backward integration, alongside the widely utilized PMS-BDD model. The results of these comparisons underscore the superior modeling efficiency of the proposed MMDD model for MS-PMS systems with dynamic phase combinations. Subsequently, considering multistate non-exponential components and the stochastic nature of phase durations, a Markov renewal equation-based method is devised to ascertain component path probabilities. Aggregating these probabilities enables the evaluation of system reliability. The proposed path evaluation methodology is juxtaposed against the Monte Carlo simulation method and the exiting approach. Comparative assessments highlight both the efficiency and accuracy of the proposed methodology. Finally, the efficacy of the proposed approach is demonstrated through a

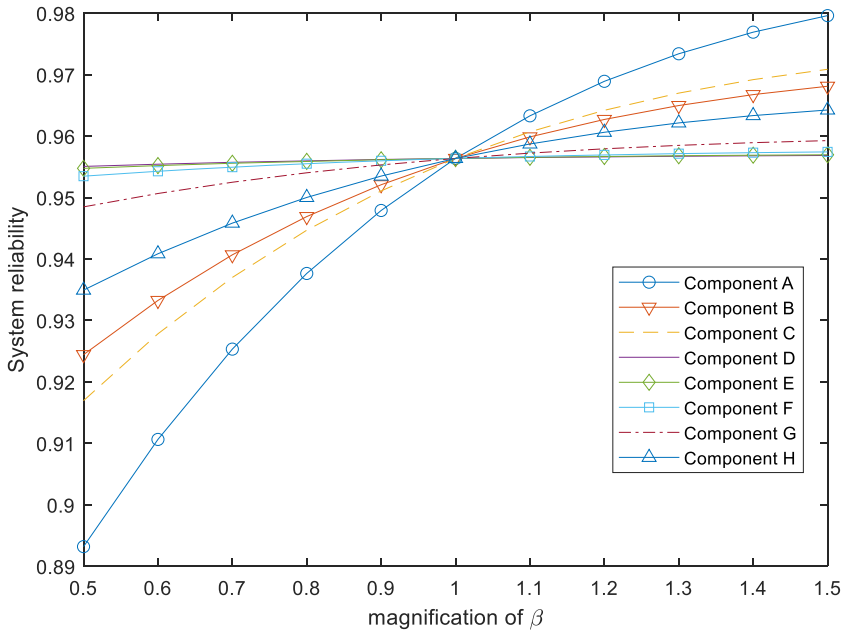

Fig. 23. Sensitivity analysis.

Table 9
Path comparison of three methods.

Paths	Proposed method	MC simulation method (2×10^6)	method in Ref [34]
η_1^C	0.945994	0.944602	0.945994
η_2^C	0.016155	0.016152	0.021538

practical application involving the Attitude and Orbit Control System of a spacecraft.

CRediT authorship contribution statement

Xiang-Yu Li: Writing – original draft, Methodology. **He Li:** Writing – review & editing, Writing – original draft, Methodology, Formal analysis. **Xiaoyan Xiong:** Validation, Methodology, Formal analysis. **Mingwei Li:** Validation, Methodology, Formal analysis. **Mohammad Yazdi:** Validation, Methodology, Formal analysis. **Esmaeil Zarei:** Writing – review & editing, Methodology.

Declaration of competing interest

There are no Conflicts of Interest.

Acknowledgements

This study is sponsored by the National Natural Science Foundation of China under Grant No. 72101173 and the Natural Science Foundation of ShanXi Province under Grant No. 20210302124442.

Data availability

Data will be made available on request.

References

[1] Li X Y, Li X, Feng J, et al. Reliability analysis and optimization of multi-phased spaceflight with backup missions and mixed redundancy strategy. Reliab. Eng. Syst. Saf. 2023;237:109373.
[2] Du S, Lin C, Cui L. Reliabilities of a single-unit system with multi-phased missions. Commun. Theory Methods 2016;45(9):2524–37.
[3] Wang D, Trivedi K S. Reliability analysis of phased-mission system with independent component repairs. IEEE Trans. Reliab. 2007;56(3):540–51.
[4] He Z, Yang J, Matsuoka T, et al. In: Reliability Analysis of Phased Mission Systems Using GO-FLOW Methodology[C]//International Conference on Nuclear Engineering. 86502. American Society of Mechanical Engineers; 2022. V015T16A059.
[5] Levitin G, Xing L, Amari S V, et al. Reliability of nonrepairable phased-mission systems with common cause failures. IEEE Trans. Syst. Man Cybernet. Syst. 2013;43(4):967–78.
[6] La Band R A, Andrews J D. Phased mission modelling using fault tree analysis. In: Proceedings of the Institution of Mechanical Engineers, Part E: Journal of Process Mechanical Engineering. 218; 2004. p. 83–91.
[7] Zang X, Sun N, Trivedi K S. A BDD-based algorithm for reliability analysis of phased-mission systems. IEEE Trans. Reliab. 1999;48(1):50–60.
[8] Kim K, Park K S. Phased-mission system reliability under Markov environment. IEEE Trans. Reliab. 1994;43(2):301–9.
[9] Zhao J, Cai Z, Si W, et al. Mission success evaluation of repairable phased-mission systems with spare part. Comput. Ind. Eng. 2019;132:248–59.
[10] Wang C, Xing L, Levitin G. Competing failure analysis in phased-mission systems with functional dependence in one of phase. Reliab. Eng. Syst. Saf. 2012;108:90–9.
[11] Wu D, Peng R, Xing L. Recent advances on reliability of phased mission systems. Stochastic Models in Reliability, Network Security and System Safety: Essays Dedicated to Professor Jinhua Cao on the Occasion of His 80th Birthday 1. 2019. p. 19–43.
[12] Xing L, Dugan J B. Analysis of generalized phased-mission system reliability, performance, and sensitivity. IEEE Trans. Reliab. 2002;51(2):199–211.
[13] Tang Z, Dugan J B. BDD-based reliability analysis of phased-mission systems with multimode failures. IEEE Trans. Reliab. 2006;55(2):350–60.
[14] Xing L. Reliability evaluation of phased-mission systems with imperfect fault coverage and common-cause failures. IEEE Trans. Reliab. 2007;56(1):58–68.
[15] Amari S V, Wang C, Xing L, et al. An efficient phased-mission reliability model considering dynamic k-out-of-n subsystem redundancy[J], 50. IISE Transactions; 2018. p. 868–77.
[16] Peng R, Zhai Q, Xing L, et al. Reliability of demand-based phased-mission systems subject to fault level coverage. Reliab. Eng. Syst. Saf. 2014;121:18–25.
[17] Lu J M, Wu X Y, Liu Y, et al. Reliability analysis of large phased-mission systems with repairable components based on success-state sampling. Reliab. Eng. Syst. Saf. 2015;142:123–33.
[18] Wu X, Wu X, Balakrishnan N. Reliability allocation model and algorithm for phased mission systems with uncertain component parameters based on importance measure. Reliab. Eng. Syst. Saf. 2018;180:266–76.
[19] Li X Y, Huang H Z, Li Y F. Reliability analysis of phased mission system with non-exponential and partially repairable components. Reliab. Eng. Syst. Saf. 2018;175:119–27.
[20] Jia X, Cao W, Hu Q. Selective maintenance optimization for random phased-mission systems subject to random common cause failures. In: Proceedings of the Institution of Mechanical Engineers, Part O: Journal of Risk and Reliability. 233; 2019. p. 379–400.
[21] Levitin G, Xing L, Xiang Y. Series phased-mission systems with heterogeneous warm standby components[J]. Comput. Ind. Eng. 2020;145:106552.
[22] Wang C, Xing L, Amari S V, et al. Efficient reliability analysis of dynamic k-out-of-n heterogeneous phased-mission systems. Reliab. Eng. Syst. Saf. 2020;193:106586.

[23] Cheng C, Yang J, Li L. Reliability evaluation of a k-out-of-n (G)-subsystem based multi-state phased mission system with common bus performance sharing subjected to common cause failures. Reliab. Eng. Syst. Saf. 2021;216:108003.
[24] Mura I. In: Stochastic Modeling and Analysis of Phased-Mission Systems Dependability[C]//2021 Annual Reliability and Maintainability Symposium (RAMS). IEEE; 2021. p. 1–6.
[25] Li X Y, Xiong X, Guo J, et al. Reliability assessment of non-repairable multi-state phased mission systems with backup missions. Reliab. Eng. Syst. Saf. 2022;223:108462.
[26] Wang C, Xing L, Su Y, et al. Reliability analysis of dynamic voting phased-mission systems. Reliab. Eng. Syst. Saf. 2023;232:109085.
[27] Coolen F P A, Huang X, Najem A. Reliability analysis of phased mission systems when components can be swapped upon failure[J]. ASCE-ASME J. Risk Uncertain. Eng. Syst. Part B: Mech. Eng. 2020;6(2):020905.
[28] Tang M, Xiahou T, Liu Y. Mission performance analysis of phased-mission systems with cross-phase competing failures. Reliab. Eng. Syst. Saf. 2023;234:109174.
[29] Levitin G, Xing L, Zonouz A E, et al. Heterogeneous warm standby multi-phase systems with variable mission time[J]. IEEE Trans. Reliab. 2015;65(1):381–93.
[30] Wang X, Xu J, Zhang L, et al. Mission success probability optimizing of phased mission system balancing the phase backup and system risk: A novel GERT mechanism. Reliab. Eng. Syst. Saf. 2023;236:109311.
[31] Li X Y, Li X, Feng J, et al. Reliability analysis and optimization of multi-phased spaceflight with backup missions and mixed redundancy strategy. Reliab. Eng. Syst. Saf. 2023;237:109373.
[32] Yu H, Wu X, Wu X. A combinatorial modeling method for mission reliability of phased-mission system with phase backups[J]. IEEE Trans. Reliab. 2020;70(2):590–601.
[33] Wu X, Yu H, Balakrishnan N. Modular model and algebraic phase algorithm for reliability modelling and evaluation of phased-mission systems with conflicting phase redundancy[J]. Reliab. Eng. Syst. Saf. 2022;227:108735.
[34] Mo Y, Siewiorek D, Yang X. Mission reliability analysis of fault-tolerant multiple-phased systems. Reliab. Eng. Syst. Saf. 2008;93(7):1036–46.